ADVANCED FUNCTIONAL MATERIALS
www.afm-journal.de

www.MaterialsViews.com

Pyridine-Containing Electron-Transport Materials for Highly Efficient Blue Phosphorescent OLEDs with Ultralow Operating Voltage and Reduced Efficiency Roll-Off

Hua Ye, Dongcheng Chen, Ming Liu, Shi-Jian Su, Yi-Fan Wang, Chang-Cheng Lo, A. Lien, and Junji Kido*

A series of pyridine-containing electron-transport materials are developed as an electron-transport layer for the FIrpic-based blue phosphorescent organic light-emitting diodes. Their energy levels can be tuned by the introduction of pyridine rings in the framework and on the periphery of the molecules. Significantly reduced operating voltage is achieved without compromising external quantum efficiency by solely tuning the nitrogen atom orientations of those pyidine rings. Unprecedented low operating voltages of 2.61 and 3.03 V are realized at 1 and 100 cd m^{-2}, giving ever highest power efficiency values of 65.8 and 59.7 lm W^{-1}, respectively. In addition, the operating voltages at 100 cd m^{-2} can be further reduced to 2.70 V by using a host material with a small singlet-triplet exchange energy, and the threshold voltage for electroluminescence can even be 0.2–0.3 V lower than the theoretical minimum value of the photon energy divided by electron charge. Aside from the reduced operating voltage, a further reduced roll-off in efficiency is also achieved by the combination of an appropriate host material.

1. Introduction

Organic light-emitting devices (OLEDs) have become of considerable commercialization interest as the next generation efficient full-color flat panel display and mercury-free lighting sources.[1] The panel efficiency of white OLEDs has recently reached 90 lm W^{-1} at 1000 cd m^{-2},[2] which is readily above the efficiency of a general fluorescent tube. However, there is still a big room for improvement compared to the theoretical limit of 248 lm W^{-1}.[3] Among the three primary colors, efficient blue light emission is the bottleneck for efficient full-color OLED display and white OLEDs.[4] In the past few years, many studies have focused on improving external quantum efficiency (h_{ext}) of blue OLEDs by utilizing a common blue phosphorescent emitter of iridium(III) bis[(4,6-difluorophenyl)-pyridinate-$N,C^{2'}$]picolinate (FIrpic). h_{ext} values over 20% have been achieved by developing new materials, such as bipolar host materials and electron-transport materials (ETMs) with high triplet energy level, due to efficient harvesting of both electro-generated singlet and triplet excitons for phosphorescent emission from OLEDs.[1c,5] Most recently, h_{ext} values were further improved to ≈30% by Lee et al. by using a pyrido[2,3-*b*]indole derivative as the host material and a 50-nm-ITO-coated glass as the substrate due to the improved carrier balance and light outcoupling.[6]

Aside from the external quantum efficiency, reducing operating voltage is also crucially important for high power conversion efficiency. As the most recent report, although h_{ext} value of ≈30% has been achieved, the power efficiency was compromised by the relatively high driving voltage, giving the maximum power efficiency (h_P) of only 50.6 lm W^{-1}.[6b] Nevertheless, unlike the most intensively investigated EQE, reducing operating voltage without compromising external quantum efficiency seems to be ignored or underestimated. The limit of operating voltage is generally believed to be equal to the energy band gap (E_g) of the emitter molecule or the photon energy ($h\nu$) of the emission light divided by the electron charge (e), which is corresponding to the energy difference between the highest occupied molecular orbital (HOMO) and the unoccupied molecular orbital (LUMO). Although a few exceptions were reported, where the devices could even be operated at half of the voltage of E_g/e,[7] the electroluminescence was achieved with an Auger-assisted mechanism, and multiple electrons should be used for one photon emission to give a very low h_{ext} of 0.4%.[7c] Actually, low driving voltage of OLEDs is generally requested without

H. Ye, D. C. Chen, M. Liu, Prof. S.-J. Su
State Key Laboratory of Luminescent Materials and Devices
Institute of Polymer Optoelectronic Materials and Devices
South China University of Technology
Guangzhou 510640, China
E-mail: mssjsu@scut.edu.cn
Y.-F. Wang, C.-C. Lo
Shenzhen China Star Optoelectronics Technology Co., Ltd
Shenzhen 518132, China
A. Lien
TCL Corporate Research,
Shenzhen 518052, China
Prof. J. Kido
Department of Organic Device Engineering
Graduate School of Science and Engineering
Yamagata University, 4–3–16 Jonan
Yonezawa, Yamagata 992–8510, Japan

DOI: 10.1002/adfm.201303785

any loss in h_{ext} to reduce their power consumption especially for high power-efficiency applications such as in mobile devices and energy-saving lighting. Note that FIrpic has a peak emission wavelength of 472 nm, which is corresponding to a photon energy (hv) of 2.63 eV. In fact, operating voltage is much higher than the value of hv/e even in state-of-the-art blue phosphorescent OLEDs.[1,5,6] Considering the highest photon energy of blue light among the three primary colors, it is challenging to achieve a blue OLED with simultaneously reduced operating voltage and improved h_{ext}, leading to further improvement of power conversion efficiency.

In this article, we report on a series of novel pyridine-containing ETMs as an electron-transport layer (ETL) of the FIrpic-based blue phosphorescent OLEDs (**Figure 1**). Their energy levels can be tuned by introducing pyridine rings with various nitrogen atom orientations on the periphery and in the framework of the molecules. Unprecedented low operating voltages of 2.61 and 3.03 V were realized at 1 and 100 cd m^{-2}, giving ever highest h_P values of 65.8 and 59.7 lm W^{-1}, respectively. Thanks to the significantly reduced operating voltages (>0.8 V) without compromising h_{ext}, the h_P values at applicable brightness of 100 and 1000 cd m^{-2} are over 30% higher than those of the device based on Tm3PyPB (1,3,5-tri(*m*-pyrid-3-yl-phenyl)benzene),[5d] one of the current best ETMs for blue phosphorescent OLEDs. In addition, further reduced operating voltages of <2.4 and 2.70 V could be achieved at 1 and 100 cd m^{-2}, respectively, by using a host material with a low singlet-triplet exchange energy (ΔE_{ST}), and the threshold voltage for electroluminescence can even be 0.2–0.3 V lower than the theoretical minimum value of hv/e. Moreover, aside from the reduced operating voltage, a further reduced efficiency roll-off was also achieved by the combination of an appropriate host material.

2. Results and Discussion

2.1. Design and Synthesis of ETMs

As an ideal ETM, it should possess a low-lying LUMO energy level to give a low electron injection barrier, a low-lying HOMO energy level to block hole leakage from the emission layer (EML), a high triplet energy level to confine triplet excitons formed in the EML, and a high electron mobility to give an effective electron transport. To match this request, several ETMs consisting of pyridine rings as the periphery in the molecules have been developed by Su et al.[5a-d] One of these multi-functional ETMs is Tm3PyPB,[5a] and it has been widely used especially for blue phosphorescent OLEDs due to its high triplet energy level and high electron mobility.[8] h_{ext} above 25% has been achieved with Tm3PyPB as an ETL as well as a hole/exciton block layer.[5a,d,8e] Although the devices based on Tm3PyPB as the ETL exhibit lower turn-on voltages (V_{on}) of 3.0~3.2 V (luminance of 1 cd m^{-2} is detected) compared with the previously reported values based on BAlq (aluminum(III) bis(2-methyl-8-quinolinato)4-phenylphenolate),[9] TPBI (2,2′,2″-(1,3,5-phenylene)tris(1-phenyl-1*H*-benzimidazole)),[10] or TAZ (3-(4-biphenyl-yl)-4-phenyl-5-(4-*tert*-butylphenyl)-1,2,4-triazole)[11] as the ETLs, there is still a large room compared to the theoretical limit of hv/e. As shown in Figure 1, a series of pyridine-containing ETMs was designed and synthesized. Synthesis details of these ETMs could be referred to Supporting Information. Different from Tm3PyPB, three more phenyls are inserted to give Tm3PyPPB, and three more pyridyls with various nitrogen atom orientations are inserted to give Tm3PyP24PyB, Tm3PyP42PyB, Tm3PyP35PyB, and Tm3PyP26PyB. Tm2PyP26PyB and Tm4PyP26PyB are analogues of Tm3PyP26PyB

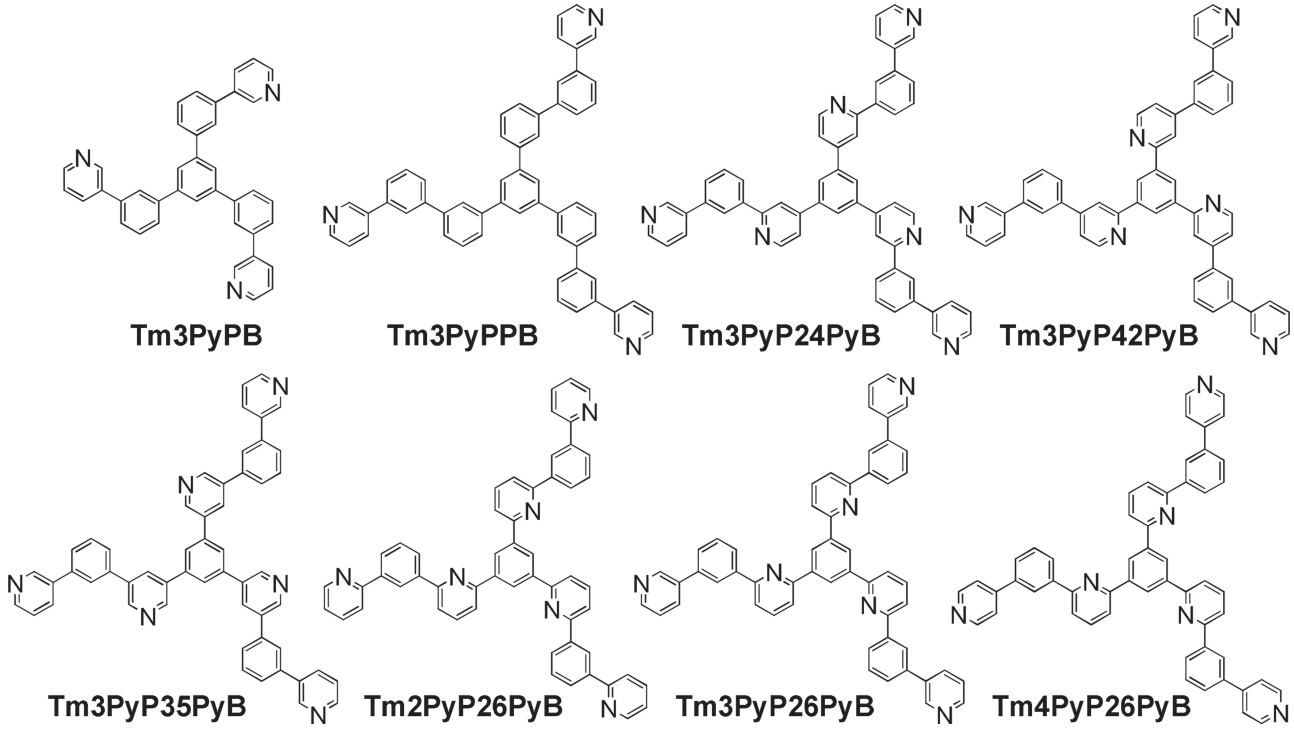

Figure 1. Molecular structures of the developed electron-transport materials. Also shown is the molecular structure of Tm3PyPB for comparison.

with the same framework but different combination sites of the peripheral pyridine rings. All the phenyls and pyridyls are combined with each other at their meta positions to give reduced π conjugation and thus high triplet energy level, and the only difference among these molecules is the number of the nitrogen atom and their orientations.

2.2. Theoretical and Experimental General Energy Levels

DFT calculations were performed using the Gaussian suite of programs (Gaussian 03W).[12] Compared with Tm3PyPB, Tm3PyPPB with three more phenyls shows slightly higher-lying HOMO and LUMO energy levels, indicating higher electron-injection barrier. In comparison, as expected, with introducing three more pyridyls into Tm3PyPB, lower-lying LUMO energy levels are achieved (**Table 1**), giving lower electron injection barrier which is preferable to a facile electron injection. Except Tm3PyP35PyB where the nitrgen atoms of the three more pyridyls are located outwards, the calculated molecular dipole moments of the compounds with three more phenyls or pyridyls are much smaller than that of Tm3PyPB (2.695 Debye), indicating smaller molecular polarity even with introduction of three more pyridine rings with strong electron affinity. The smallest dipole moment is obtained for Tm3PyP26PyB, and it is preferable to a facile electron transport. Aside from the pyridine rings combined with the benzene core, the energy levels are also strongly dependent on the nitrogen orientations of the peripheral pyridine rings. Lower-lying HOMO and LUMO energy levels are obtained when the nitrogen position of the peripheral pyridine rings changes from 2 to 3 and 4 for the compounds with the same framework.

The experimental results indicate that Tm3PyPPB with three more phenyls shows a higher-lying LUMO energy level (the same value as the electron affinity (E_a) shown in **Table 2**) of –2.59 eV compared to Tm3PyPB (LUMO = –2.73 eV).[5a] Consistent with the DFT calculations, lower-lying LUMO energy levels are achieved with introducing three pyridyls instead of those three phenyls, and the LUMO energy levels of Tm3PyP24PyB and Tm3PyP26PyB are further lower-lying than those of the other two analogues of Tm3PyP42PyB and Tm3PyP35PyB. In addition, LUMO energy level of Tm3PyP35PyB (–2.66 eV) is the highest one among the compounds consisting of six pyridine rings, and it is even higher-lying than that of Tm3PyPB. Similar to the DFT calculations, for the compounds with the same framework, lower-lying HOMO and LUMO energy levels are obtained in the order of Tm2PyP26PyB, Tm3PyP26PyB, and Tm4PyP26PyB, where the nitrogen position of the peripheral pyridine rings changes from 2 to 3 and 4. Although the exact values are somewhat different from the calculated one since the theoretically estimated one is in gas phase with isolated molecules in contrast to experimentally estimated one in condense phase, the tendency of the experimentally estimated energy levels is well consistent with that of the theoretically estimated one.

Another important factor for ETM that may affect the device performance is its triplet energy level (E_T). As suggested by the DFT calculations, triplet energy levels of the designed ETMs are affected slightly compared with the HOMO and LUMO energy levels and dipole moments. It is suspected that the triplet energy of Tm3PyP26PyB is the lowest one among these newly developed ETMs and Tm3PyPB. Thereby, Tm3PyP26PyB is chosen as one typical material to access weather its triplet energy is high enough for the confinement of triplet excitons generated on the phosphor of FIrpic. The delayed component (2 ms < t < 10 ms) of the time-resolved emission spectrum for the vacuum-deposited film of Tm3PyP26PyB on quartz substrate is not so clear to estimate its triplet energy, due to the big signal noise and the unavoidable delayed fluorescence emission even at a very low temperature of 4.2 K (Figure S4, Supporting Information). Although the molecular skeletons are rather extended through the meta-conjugation compared with Tm3PyPB, we have found that the compounds with similarly extended meta-conjugation have higher triplet energy compared with the blue phosphor of FIrpic.[13] It is speculated that triplet energies of the current ETMs should also be high enough for triplet exciton confinement of the generally used phosphorescent emitter FIrpic. To verify its triplet exciton confinement ability, FIrpic (3 wt%) was co-deposited with Tm3PyP26PyB for transient PL decay measurement. Although the transient photoluminescence decay is not monoexponential (Figure S5, Supporting Information),

Table 1. Density functional theory (DFT) calculations of the developed electron-transport materials.[a)]

Materials	HOMO [eV]	LUMO [eV]	E_g^{cal} [eV]	$T_1 - S_0$ [eV]	Dipole Moment [D]
Tm3PyPB	–6.46	–1.64	4.82	2.95	2.695
Tm3PyPPB	–6.38	–1.60	4.78	2.97	1.216
Tm3PyP24PyB	–6.64	–2.21	4.44	2.91	1.065
Tm3PyP42PyB	–6.40	–1.91	4.48	2.88	1.081
Tm3PyP35PyB	–6.69	–1.90	4.79	2.96	2.602
Tm2PyP26PyB	–6.11	–1.71	4.40	2.89	0.609
Tm3PyP26PyB	–6.35	–1.89	4.46	2.84	0.459
Tm4PyP26PyB	–6.46	–2.00	4.45	2.84	0.646

[a)]Molecular structure optimization and single-point energy calculations were performed at B3LYP/6–31G(d) and B3LYP/6–311+G(d,p) levels (DFT, Gaussian 03W), respectively.

Table 2. Physical properties of the developed electron-transport materials.

Materials	T_g [°C][a)]	T_m [°C][a)]	T_d [°C][b)]	λ_{PL} [nm][c)]	IP [eV][d)]	E_a [eV][e)]	E_g^{opt} [eV][f)]
Tm3PyPPB	99.2	n.a.	493	352	6.67	2.59	4.08
Tm3PyP24PyB	118	n.a.	502	380	6.68	2.93	3.75
Tm3PyP42PyB	111	248	511	384	6.61	2.82	3.79
Tm3PyP35PyB	124	257	509	357	6.63	2.66	3.97
Tm2PyP26PyB	97.8	234	521	371	6.34	2.74	3.60
Tm3PyP26PyB	91.3	234	509	374	6.50	2.91	3.59
Tm4PyP26PyB	115	267	517	373	6.63	3.04	3.59

[a)]Glass transition temperature (T_g) and melting temperature (T_m) obtained from differential scanning calorimetry (DSC) measurement; [b)]Decomposition temperature (T_d) obtained from thermogravimetric analysis (TGA); [c)]Photoluminescence spectrum of vacuum deposited film on quartz substrate; [d)]Ionization potential (IP) determined by atmospheric ultraviolet photoelectron spectroscopy (Rikken Keiki AC-3); [e)] Electron affinity (E_a) calculated from IP and E_g^{opt}; [f)]Optical energy band gap (E_g^{opt}) from the lowest-energy absorption edge of the UV-vis absorption spectrum.

similar to the co-deposited film of Tm3PyPB:FIrpic (3 wt%),[5d] its second exponential decay part (4.7%) is much smaller than its first (95.3%), indicating the triplet energy transfer from FIrpic is successfully suppressed by Tm3PyP26PyB. As thus, it suggests that the triplet energy level of Tm3PyP26PyB is higher or, at least, comparable to that of FIrpic. This is quite important if it is to be used as an exciton block layer to confine the FIrpic triplet excitons within the emissive layer to achieve an efficient blue phosphorescent OLED.

2.3. Thermal Properties

As shown in Table 2, the materials with six pyridine rings show relatively higher glass transition temperature (T_g), melting temperature (T_m), and decomposition temperature (T_d) than Tm3PyPPB except Tm2PyP26PyB and Tm3PyP26PyB. The lowest T_g was obtained for Tm3PyP26PyB, and it may be attributed to the weakest intermolecular interaction as proven by the smallest dipole moment obtained by the DFT calculations. Nevertheless, it is still 12 °C higher than that of Tm3PyPB (T_g = 79 °C).[5a]

AFM measurement was conducted to investigate the surface topography of the developed ETMs in solid state thin films before and after thermal annealing. All these thin films show a flat surface before and after thermal annealing, with a root-mean-squared (RMS) roughness below 1.5 nm (Figure S6, Supporting Information). However, some grains were found after thermal annealing for the thin films of Tm3PyP24PyB, Tm3PyP42PyB, and Tm4PyP26PyB. Some of the pyridine rings in these molecules are combined at their para site of the nitrogen atom, and it may induce an improved intermolecular interaction and thus self-aggregation during the thermal treatment. In contrast, for the thin films of Tm3PyPB, Tm3PyP26PyB, and Tm3PyP35PyB that have T_g values of 79, 91.3, and 124 °C, respectively, stable amorphous morphology keeps well after thermal annealing, indicating that the molecular structure dominates the morphological stability rather than T_g.

2.4. Phosphorescent OLEDs

Although the devices based on FIrpic were reported with lifetime issue,[1c,d] as the mostly investigated blue phosphorescent emitter, it was also used in the current blue phosphorescent OLEDs to evaluate the developed ETMs as an undoped ETL without inserting any other hole or exciton-block layer between the EML and ETL. For comparison, a reference device was also fabricated by using Tm3PyPB as an ETL. TPDPES (poly(arylene amine ether sulfone)-containing tetraphenylbenzidine) blended with 10% (by weight) TBPAH (tris(4-bromophenyl) aminium hexachloroantimonate) was used as the anode buffer layer to improve the hole injection. TAPC (1,1-bis[4-[N,N-di(*p*-tolyl)-amino]phenyl]cyclohexane) and 26DCzPPy (2,6-bis(3-(carbazol-9-yl)phenyl)pyridine) were used as the hole-transport material and host material, respectively. Well-known cathode consisting of a 0.5-nm-thick layer of LiF followed by a 100-nm-thick layer of Al was patterned using a shadow mask with an array of 2 mm × 2 mm openings.

Driving voltage of the device based on Tm3PyPPB is slightly higher than that of the device based on Tm3PyPB (**Figure 2**a), and it can be attributed to its higher-lying LUMO energy level compared with Tm3PyPB. As a result, h_{ext} of the device based on Tm3PyPPB is slightly lower than that of the device based on Tm3PyPB due to the reduced carrier balance. By inserting three more pyridyls into Tm3PyPB, clearly reduced driving voltage is achieved except Tm3PyP35PyB, and it is of interest the driving voltage is significantly dependent on the nitrogen atom orientations of those pyridine rings. Among these four analogues, LUMO energy level of Tm3PyP35PyB is obviously higher-lying than those of the others. As thus, driving voltage of the device based on Tm3PyP35PyB is also obviously higher than those of the devices based on the others. Thanks to the lower-lying LUMO energy level and the smallest dipole moment of Tm3PyP26PyB, the lowest driving voltage is achieved by Tm3PyP26PyB. An extremely low V_{on} of 2.60 V is achieved for electroluminescence, which is 0.64 V lower than that of the device based on Tm3PyPB (V_{on} = 3.24 V) and is readily comparable to the minimum value of $h\nu/e$. At a display-relevant luminance of 100 cd m^{-2}, the operating voltage is only 3.03 V, and it is 0.8 V lower than that of the device based on Tm3PyPB. Even at an illumination-relevant luminance of 1000 cd m^{-2}, the operating voltage is as low as 3.47 V, and it is reduced by 1.0 V compared with the device based on Tm3PyPB. Consistent with the order of LUMO energy levels and the dipole moments, the driving

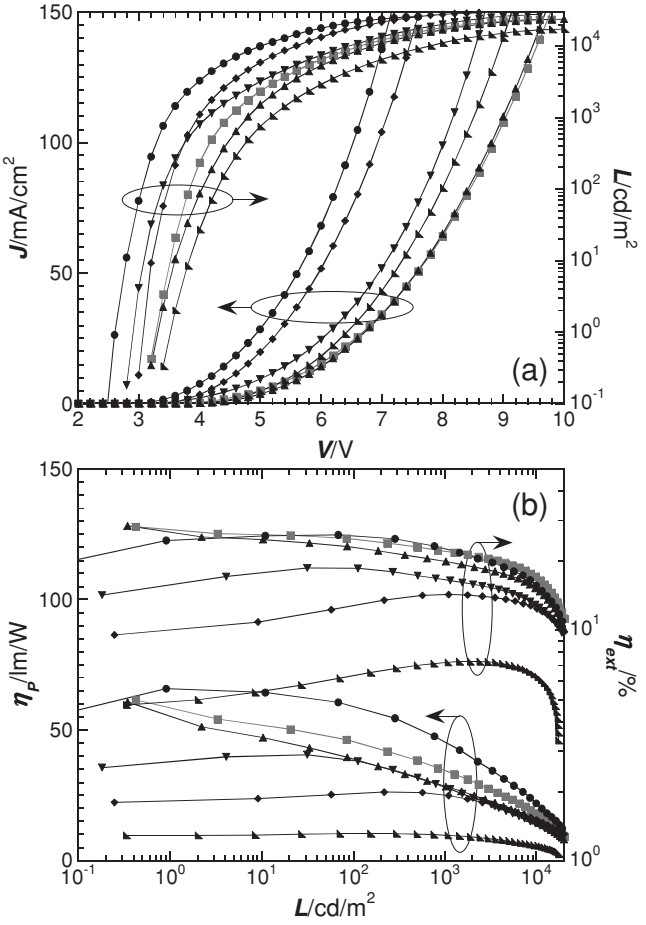

Figure 2. a) Current density (*J*) and luminance (*L*) versus operating voltage and b) power efficiency (h_P) and external quantum efficiency (h_{ext}) versus luminance characteristics of the devices in a structure of ITO/TPDPES (20 nm)/TAPC (30 nm)/26DCzPPy : 13 wt% FIrpic (10 nm)/ETL (50 nm)/LiF (0.5 nm)/Al (100 nm). ETL: Tm3PyPB (■), Tm3PyPPB (▲), Tm3PyP24PyB (▼), Tm3PyP42PyB (◆), Tm3PyP35PyB (◣), or Tm3PyP26PyB (●).

voltages of the devices based on Tm3PyP24PyB and Tm3PyP42PyB are between those of the devices based on Tm3PyP26PyB and Tm3PyP35PyB.

Electron-only devices with a configuration of ITO/LiF (1 nm)/ETM (50 nm)/LiF (1 nm)/Al (100 nm) were also fabricated to investigate the electron-transport behavior of these ETMs. It is observed that the current density for the electron-only device based on Tm3PyPB is smaller than the other ETMs consisting of three more pyridine rings, which may be attributed to its higher-lying LUMO energy level and lower electron mobility. The tendency of the current density for the ETMs with different nitrogen atom orientations of those pyridine rings is different from those of the corresponding phosphorescent OLEDs, and it may be attributed to the different hole current in those devices.

Aside from the significantly reduced driving voltage, h_{ext} as high as 25.7% is achieved at 100 cd m^{-2} by using Tm3PyP26PyB as the ETL, which is comparable with that of the device based on Tm3PyPB (24.9%). The current h_{ext} is a little lower than the ever highest one[6b] maybe due to the 60-nm-thicker ITO (110 nm vs 50 nm), which has a lower transmittance in blue wavelength range[14] and may induce a lower light outcoupling efficiency.[15] However, it is still one of the highest values based on the same thickness ITO substrate. In addition, it shows a h_{ext} of 22.6% at an illumination-relevant luminance of 1000 cd m^{-2}, which is over 87% of the maximum h_{ext} (25.9%) in comparison with 84% for the Tm3PyPB-based device, indicating a reduced efficiency roll-off. Considering the reduced driving voltage and improved carrier balance, hole-injection and transport must be simultaneously improved although the same anode buffer layer and hole-transport layer were used. It is speculated that the improved electron injection may induce an aggregation of electron at the cathode side and thus an increased internal electric field and the hole injection and transport from the anode should thus be accelerated due to the increased electric field. Besides the improved carrier balance, good confinement of the triplet excitons within the EML by Tm3PyP26PyB should also contribute to the improved h_{ext}. Due to the significantly reduced driving voltage without compromising h_{ext}, a maximum h_P of 65.8 lm W^{-1} is achieved at 1 cd m^{-2}, and hitherto the highest h_P values of 59.7 and 45.8 lm W^{-1} are achieved at applicable brightness of 100 and 1000 cd m^{-2}, respectively, which are over 30% higher than those of the device based on Tm3PyPB. As shown in Figure 2b, the device efficiencies are also significantly dependent on the nitrogen atom orientations of the three more pyridine rings. Fairly low h_P of 10.2 lm W^{-1} and h_{ext} of 6.29% are obtained at 100 cd m^{-2} for the device based on Tm3PyP35PyB. Different from the other devices, a very weak emission band at 394 nm was observed for the electroluminescent (EL) spectrum of this device, and it can be attributed to the emission from the ETL of Tm3PyP35PyB (See Supplementary Information). The carriers should be recombined at the interface of EML and ETL for this device to give the low device performance. In comparison, efficiencies of the devices based on Tm3PyP24PyB and Tm3PyP42PyB are between those of the devices based on Tm3PyP26PyB and Tm3PyP35PyB. Their relatively lower efficiency compared with the device based on Tm3PyP26PyB may be attributed to the reduced carrier balance.

Besides the nitrogen atom orientations of the inside pyridine rings of the molecules, the device performance is also dependent on the nitrogen atom orientations of the peripheral pyridine rings. As shown in **Figure 3**(a), for the ETMs with the same framework, current density increases when the nitrogen position of the peripheral pyridine rings changes from 2 to 3 and 4. Consistent with the light-emitting devices, the electron current also increases when the nitrogen position of the peripheral pyridine rings changes from 2 to 3 and 4 for the corresponding electron-only devices, and it can be attributed to the lower-lying LUMO energy level and thus decreased electron injection barrier in the same order. On this result, the driving voltage of the device based on Tm4PyP26PyB is even lower than that of the device based on Tm3PyP26PyB at applicable brightness. However, relatively lower h_{ext} values of 20.6% and 19.3% are obtained at 100 and 1000 cd m^{-2}, respectively, due to the reduced carrier balance. Although the h_{ext} values are lower than those of the device based on Tm3PyPB, higher h_P values of 47.2 and 40.0 lm W^{-1} are achieved at 100 and 1000 cd m^{-2}, respectively, because of the reduced driving voltage. It is also interesting h_{ext} of the device based on Tm2PyP26PyB is almost the same as that of the device based on Tm3PyP26PyB although

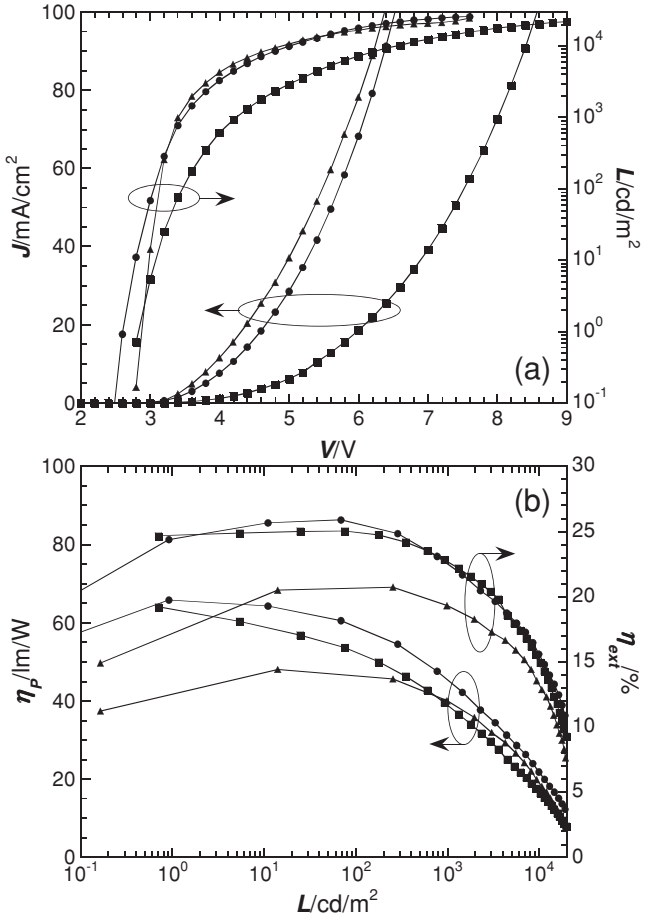

Figure 3. a) Current density (*J*) and luminance (*L*) versus operating voltage and b) power efficiency (h_P) and external quantum efficiency (h_{ext}) versus luminance characteristics of the devices in a structure of ITO/TPDPES (20 nm)/TAPC (30 nm)/26DCzPPy : 13 wt% FIrpic (10 nm)/ETL (50 nm)/LiF (0.5 nm)/Al (100 nm). ETL: Tm2PyP26PyB (■), Tm3PyP26PyB (●), or Tm4PyP26PyB (▲).

its driving voltage is much higher. It further proves the hole injection and transport could be tuned by the use of an appropriate ETM to give a good carrier balance as well as a reduced driving voltage. Compared with the previously reported ETM of Tm2PyPB (1,3,5-tri(*m*-pyrid-2-ylphenyl)benzene)[5d] with the same combination site of the peripheral pyridine rings but different framework, the current device based on Tm2PyP26PyB exhibits simultaneously reduced driving voltages of 3.45 and 4.23 V, improved h_{ext} values of 25.0% and 22.8%, and improved h_P values of 52.7 and 39.0 lm W^{-1} at 100 and 1000 cd m^{-2}, respectively. Similar phenomenon was also found for Tm4PyP26PyB compared with Tm4PyPB (1,3,5-tri(*m*-pyrid-4-ylphenyl)benzene),[5d] further indicating the device performance is heavily dependent on the framework of the ETM molecules besides the peripheral pyridine.

Besides ETMs, driving voltage can be further reduced by changing the host material used for FIrpic although the EML is as thin as 10 nm. As shown in **Figure 4** (left), for the bis-carbazole host materials, the driving voltage can be reduced in the order of DCzPB (1,3-bis(3-(carbazol-9-yl)phenyl)benezene), 26DCzPPy, and 46DCzPPm (4,6-bis(3-(carbazol-9-yl)phenyl)pyrimidine). The

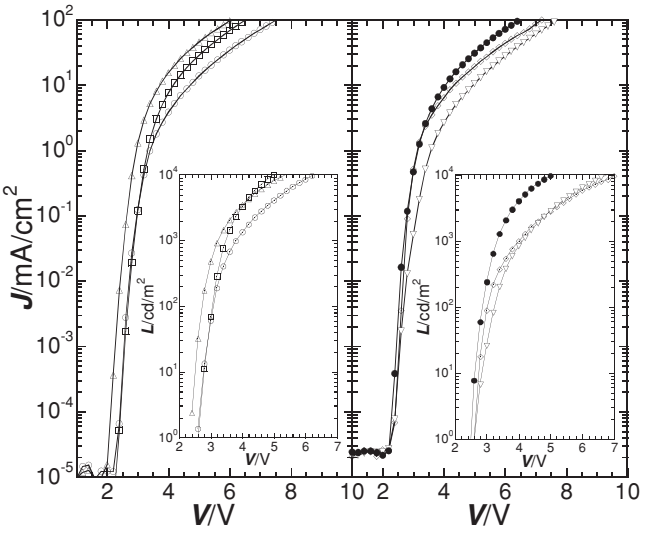

Figure 4. Current density (*J*) and luminance (*L*, inset) versus operating voltage characteristics of the devices in a structure of ITO/TPDPES (20 nm)/TAPC (30 nm)/Host : 13 wt% FIrpic (10 nm)/Tm3PyP26PyB (50 nm) /LiF (0.5 nm) /Al (100 nm). Host: DCzPB (○), 26DCzPPy (□), 46DCzPPm (△), TCTA (◇), TCPB (▽), or TCPY (●).

reduced driving voltage should be attributed to the lower-lying LUMO energy level and the narrower singlet-triplet exchange energy (ΔE_{ST}) for the host materials in the same order (See Supplementary Information). Ultralow driving voltage is achieved for the device based on 46DCzPPm, giving a threshold voltage of ≈2.0 V for current and a V_{on} of <2.4 V for electroluminescence. It is of interest that the threshold voltage for electroluminescence can even be 0.2–0.3 V lower than the minimum value of *hv*/*e*. At a display-relevant luminance of 100 cd m^{-2}, the operating voltage is only 2.70 V, and it is 0.33 V lower than that of the device based on 26DCzPPy and is very near the minimum value of *hv*/*e*. As supposed by Meerheim et al., in an ideal device the quasi-Fermi-level spread is identical to the voltage applied to the contacts of the device, the thermodynamic limit of the operating voltage in a blue OLED is estimated to be ≈2.28 V at 100 cd m^{-2} by the use of an equation based on black-body radiation, and it is the highest one among the three primary colors.[16] Considering the exciton binding energy might need some extra energy (depending on whether there is resonant exciton generation), it is also interesting that the operating voltages currently achieved experimentally are already very close to the thermodynamic limits at low brightness. However, the voltages at higher brightness are nevertheless higher than the thermodynamic limits, and it is another challenge to further improve OLEDs so that very steep exponential luminance curves can be achieved with OLEDs as well.

Note that E_Ts of these bis-carbazole host materials are high enough for efficient energy transfer from the host to the guest and good confinement of the triplet energy on the FIrpic molecules.[17] Relatively lower h_{ext} values of the devices based on DCzPB and 46DCzPPm could be attributed to the reduced carrier balance (See Supplementary Information). In addition, considering the relatively lower photoluminescent quantum efficiency (h_{PL}) of FIrpic doped in 46DCzPPm (h_{PL} = 0.73 ± 0.01) than that of DCzPB:FIrpic (h_{PL} = 0.83 ± 0.01) and 26DCzPPy:FIrpic (h_{PL} = 0.84 ± 0.01), further lower h_{ext} is

obtained for the device based on 46DCzPPm. However, thanks to the ultralow driving voltage, high h_P over 50 lm W^{-1} is still achieved at 100 cd m^{-2} (**Table 3**).

For the tris-carbazole host materials, the driving voltage can be reduced in the order of TCPB (1,3,5-tris(3-(carbazol-9-yl)phenyl)-benzene), TCTA (4,4′,4″-tri(*N*-carbazolyl)triphenylamine), and TCPY (2,4,6-tris(3-(carbazol-9-yl)phenyl)-pyridine) (Figure 4, right). Note that TCTA consisting of triphenylamine core is a well-known hole-transport host material. Compared with the device based on TCPB, current density of the device based on TCTA is much higher, but giving comparable brightness. It can be attributed to the excess hole current and thus significantly reduced carrier balance. In contrast, TCPY is an ambipolar host material due to its similar hole and electron mobilities.[18] As a result, clearly higher h_{ext} values of 22.3% and 22.4% are achieved at 100 and 1000 cd m^{-2}, respectively, for the device based on TCPY. Although the h_{ext} values for the device based on TCPY are somewhat lower than those of the device based on 26DCzPPy with the same pyridine core, considering the relatively lower h_{PL} of TCPY:FIrpic ($h_{PL} = 0.72 \pm 0.01$) than that of 26DCzPPy:FIrpic and light outcoupling efficiency of ≈30% in a similar device architecture without using any light outcoupling enhancement techniques, well balanced carriers are also achieved for the device based on TCPY and Tm3PyP26PyB. In addition, compared with the device based on 26DCzPPy whose h_{ext} value at 1000 cd m^{-2} is 87% of the maximum h_{ext}, the h_{ext} values at 100 and 1000 cd m^{-2} are almost the same as the maximum h_{ext} (22.7%) for the device based on TCPY, indicating a further reduced roll-off in efficiency, and this is very important for high brightness applications like lighting. Moreover, reduced driving voltages of 2.85 and 3.31 V are also achieved at 100 and 1000 cd m^{-2}, giving extremely high h_P values of 55.5 and 47.8 lm W^{-1}, respectively, and it can be attributed to the lower-lying LUMO energy level and the small ΔE_{ST} of TCPY and thus improved electron injection from the ETL.

3. Conclusions

In summary, a series of pyridine-containing ETMs were developed as an ETL of the FIrpic-based blue phosphorescent OLEDs. By tuning their energy levels with introduction of pyridine rings with various nitrogen atom orientations on the periphery and in the framework of the molecules, unprecedented low operating voltages of 2.61 and 3.03 V were realized at 1 and 100 cd m^{-2}, giving ever highest h_P values of 65.8 and 59.7 lm W^{-1} and h_{ext} values of 24.4% and 25.7%, respectively. In addition, further reduced operating voltages of <2.4 and 2.70 V were achieved at 1 and 100 cd m^{-2}, respectively, by using a host material of 46DCzPPm with a small E_{ST}, and the threshold voltage for electroluminescence can even be 0.2–0.3 V lower than the theoretical minimum value of $h\nu/e$. Moreover, a further reduced efficiency roll-off was achieved by using TCPY as the host material, and this is an important factor for high brightness applications like lighting. Considering no chemical doping was used for the ETL of the current devices, there might be still some further room to reduce the driving voltage by using chemically doping technology.[19] In addition, the driving voltage may also be further reduced by utilizing double host materials[20] or double EMLs[1c,5b] to tune the carrier injection barrier between the EML and the carrier transport layer. These low operating voltage devices makes them very interesting for high power-efficiency applications such as in mobile devices and organic lighting.

4. Experimental Section

Materials: Synthetic details and chararacterizations of newly developed ETMs, including Tm3PyPPB, Tm3PyP24PyB, Tm3PyP42PyB, Tm3PyP35PyB, Tm2PyP26PyB, Tm3PyP26PyB, and Tm4PyP26PyB, are demonstrated in Supplementary Information. Tm3PyPB,[5a] DCzPB,[17] 26DCzPPy,[21] 46DCzPPm,[17] TCPB,[18] and TCPY[18] were synthesized according to the procedures reported in the literatures. All the materials used for device fabrication were purified by repeated temperature gradient vacuum sublimation.

Table 3. Summary of the OLED performances of the devices in a structure of ITO/TPDPES (20 nm)/TAPC (30 nm)/Host : 13 wt% FIrpic (10 nm)/ETL (50 nm)/LiF (0.5 nm)/Al (100 nm).

ETL	Host	Performance at 100 cd m^{-2} $V/h_P/h_{ext}$ [V lm^{-1} W^{-1}/%]	Performance at 1000 cd m^{-2} $V/h_P/h_{ext}$ [V lm^{-1} W^{-1}/%]
Tm3PyPB	26DCzPPy	3.82/45.7 ± 0.9/24.9 ± 0.5	4.47/34.5 ± 0.7/22.0 ± 0.4
Tm3PyPPB		4.03/39.0 ± 0.7/22.8 ± 0.5	4.78/28.5 ± 0.5/19.8 ± 0.4
Tm3PyP24PyB		3.37/38.4 ± 0.8/18.5 ± 0.4	4.12/28.1 ± 0.6/16.5 ± 0.3
Tm3PyP42PyB		3.45/25.4 ± 0.5/12.6 ± 0.3	3.96/25.0 ± 0.5/14.2 ± 0.3
Tm3PyP35PyB		4.27/10.2 ± 0.2/6.29 ± 0.1	5.16/9.70 ± 0.2/7.22 ± 0.1
Tm2PyP26PyB		3.45/52.7 ± 0.9/25.0 ± 0.5	4.23/39.0 ± 0.8/22.8 ± 0.4
Tm3PyP26PyB		3.03/59.7 ± 0.9/25.7 ± 0.5	3.47/45.8 ± 0.9/22.6 ± 0.4
Tm4PyP26PyB		3.07/47.2 ± 0.9/20.6 ± 0.4	3.40/40.0 ± 0.8/19.3 ± 0.4
Tm3PyP26PyB	DCzPB	3.06/48.8 ± 0.9/21.4 ± 0.4	3.81/29.8 ± 0.6/16.3 ± 0.3
	46DCzPPm	2.70/50.3 ± 0.9/17.4 ± 0.3	3.23/30.2 ± 0.6/12.5 ± 0.2
	TCTA	3.02/17.9 ± 0.3/7.60 ± 0.1	4.01/12.1 ± 0.2/6.79 ± 0.1
	TCPB	3.23/43.9 ± 0.8/20.2 ± 0.4	4.11/23.5 ± 0.4/13.7 ± 0.2
	TCPY	2.85/55.5 ± 0.9/22.3 ± 0.4	3.31/47.8 ± 0.9/22.4 ± 0.4

Calculation: For calculation of HOMO and LUMO energy levels, DFT calculations were performed for optimized molecular structures and single-point energies at the B3LYP/6–31G(d) and B3LYP/6–311+G(d,p) levels, respectively, using the Gaussian suite of programs (Gaussian 03W). For calculation of ground (S_0) and triplet excited states (T_1), optimized molecular structures and single-point energies were also calculated at the B3LYP/6–31G(d) and B3LYP/6–311+G(d,p) levels, respectively.

Supporting Information

Supporting Information is available from the Wiley Online Library or from the author.

Acknowledgements

H.Y. and D.C.C. contributed equally to this work. S.J.S. greatly appreciates the financial support from the National Natural Science Foundation of China (51073057 and 91233116), the Ministry of Science and Technology (2011AA03A110), the Ministry of Education (NCET-11–0159), and the Fundamental Research Funds for the Central Universities (2013ZG0007).

Received: November 8, 2013
Revised: December 12, 2013
Published online: February 4, 2014

[1] a) J. Kido, M. Kimura, K. Nagai, **1995**, *267*, 1332; b) Y. Sun, N. C. Giebink, H. Kanno, B. Ma, M. E. Thompson, S. R. Forrest, *Nature* **2006**, *440*, 908; c) S.-J. Su, E. Gonmori, H. Sasabe, J. Kido, *Adv. Mater.* **2008**, *20*, 4189; d) S. Reineke, F. Lindner, G. Schwartz, N. Seidler, K. Walzer, B. Lussem, K. Leo, *Nature* **2009**, *459*, 234.

[2] T. Komoda, K. Yamae, V. Kittichungchit, H. Tsuji, N. Ide, *SID 12 Dig.* **2012**, 610.

[3] a) Y. Ohno, *Opt. Eng.* **2005**, *44*, 111302; b) Y.-S. Tyan, *J. Photonics Energy* **2011**, *1*, 011009.

[4] a) B. W. D'Andrade, R. J. Holmes, S. R. Forrest, *Adv. Mater.* **2004**, *16*, 624; b) Y. Sun, S. R. Forrest, *Appl. Phys. Lett.* **2007**, *91*, 263503.

[5] a) S.-J. Su, T. Chiba, T. Takeda, J. Kido, *Adv. Mater.* **2008**, *20*, 2125; b) H. Sasabe, E. Gonmori, T. Chiba, Y.-J. Li, D. Tanaka, S.-J. Su, T. Takeda, Y.-J. Pu, K.-I. Nakayama, J. Kido, *Chem. Mater.* **2008**, *20*, 5951; c) L. Xiao, S.-J. Su, Y. Agata, H. Lan, J. Kido, *Adv. Mater.* **2009**, *21*, 1271; d) S.-J. Su, Y. Takahashi, T. Chiba, T. Takeda, J. Kido, *Adv. Funct. Mater.* **2009**, *19*, 1260; e) H. Sasabe, N. Toyota, H. Nakanishi, T. Ishizaka, Y.-J. Pu, J. Kido, *Adv. Mater.* **2012**, *24*, 3212; f) J. K. Bin, N. S. Cho, J. I. Hong, *Adv. Mater.* **2012**, *24*, 2911; g) M. S. Lin, S. J. Yang, H. W. Chang, Y. H. Huang, Y. T. Tsai, C. C. Wu, S. H. Chou, E. Mondal, K. T. Wong, *J. Mater. Chem.* **2012**, *22*, 16114.

[6] a) C. W. Lee, Y. Im, S. A. Seo, J. Y. Lee, *Chem. Commun.* **2013**, *49*, 9860; b) C. W. Lee, J. Y. Lee, *Adv. Mater.* **2013**, *25*, 5450.

[7] a) A. C. Morteani, A. S. Dhoot, J.-S. Kim, C. Silva, N. C. Greenham, C. Murphy, E. Moons, S. Ciná, J. H. Burroughes, R. H. Friend, *Adv. Mater.* **2003**, *15*, 1708; b) A. K. Pandey, J. M. Nunzi, *Adv. Mater.* **2007**, *19*, 3613; c) L. Qian, Y. Zheng, K. R. Choudhury, D. Bera, F. So, J. Xue, P. H. Holloway, *Nano Today* **2010**, *5*, 384.

[8] a) J. H. Lee, J.-I. Lee, J. Y. Lee, H. Y. Chu, *Appl. Phys. Lett.* **2009**, *94*, 193305; b) H. Fukagawa, S. Irisa, H. Hanashima, T. Shimizu, S. Tokito, N. Yokoyama, H. Fujikake, *Org. Electron.* **2011**, *12*, 1638; c) S. L. Gong, Q. Fu, Q. Wang, C. L. Yang, C. Zhong, J. G. Qin, D. G. Ma, *Adv. Mater.* **2011**, *23*, 4956; d) C.-W. Hsu, C.-C. Lin, M.-W. Chung, Y. Chi, G.-H. Lee, P.-T. Chou, C.-H. Chang, P.-Y. Chen, *J. Am. Chem. Soc.* **2011**, *133*, 12085; e) G. Méhes, H. Nomura, Q. S. Zhang, T. Nakagawa, C. Adachi, *Angew. Chem. Int. Ed.* **2012**, *51*, 11311.

[9] a) R. J. Holmes, S. R. Forrest, Y.-T. Tung, R. C. Kwong, J. J. Brown, S. Garon, M. E. Thompson, *Appl. Phys. Lett.* **2003**, *82*, 2422; b) S. Tokito, T. Iijima, Y. Suzuki, H. Kita, T. Tsuzuki, F. Sato, *Appl. Phys. Lett.* **2003**, *83*, 569.

[10] a) S.-J. Yeh, M.-F. Wu, C.-T. Chen, Y.-H. Song, Y. Chi, M.-H. Ho, S.-F. Hsu, C. H. Chen, *Adv. Mater.* **2005**, *17*, 285; b) D. H. Yu, F. C. Zhao, C. M. Han, H. Xu, J. Li, Z. Zhang, Z. P. Deng, D. G. Ma, P. F. Yan, *Adv. Mater.* **2012**, *24*, 509.

[11] a) M.-H. Tsai, H.-W. Lin, H.-C. Su, T. H. Ke, C.-C. Wu, F.-C. Fang, Y.-L. Liao, K.-T. Wong, C.-I. Wu, *Adv. Mater.* **2006**, *18*, 1216; b) C. H. Cheng, H. H. Chou, *Adv. Mater.* **2010**, *22*, 2468.

[12] M. J. Frisch, G. W. Trucks, H. B. Schlegel, G. E. Scuseria, M. A. Robb, J. R. Cheeseman, J. A. Montgomery Jr. , T. Vreven, K. N. Kudin, J. C. Burant, J. M. Millam, S. S. Iyengar, J. Tomasi, V. Barone, B. Mennucci, M. Cossi, G. Scalmani, N. Rega, G. A. Petersson, H. Nakatsuji, M. Hada, M. Ehara, K. Toyota, R. Fukuda, J. Hasegawa, M. Ishida, T. Nakajima, Y. Honda, O. Kitao, H. Nakai, M. Klene, X. Li, J. E. Knox, H. P. Hratchian, J. B. Cross, V. Bakken, C. Adamo, J. Jaramillo, R. Gomperts, R. E. Stratmann, O. Yazyev, A. J. Austin, R. Cammi, C. Pomelli, J. W. Ochterski, P. Y. Ayala, K. Morokuma, G. A. Voth, P. Salvador, J. J. Dannenberg, V. G. Zakrzewski, S. Dapprich, A. D. Daniels, M. C. Strain, O. Farkas, D. K. Malick, A. D. Rabuck, K. Raghavachari, J. B. Foresman, J. V. Ortiz, Q. Cui, A. G. Baboul, S. Clifford, J. Cioslowski, B. B. Stefanov, G. Liu, A. Liashenko, P. Piskorz, I. Komaromi, R. L. Martin, D. J. Fox, T. Keith, M. A. Al-Laham, C. Y. Peng, A. Nanayakkara, M. Challacombe, P. M. W. Gill, B. Johnson, W. Chen, M. W. Wong, C. Gonzalez, J. A. Pople, *Gaussian 03*, *Revision D.01*, Gaussian, Inc., Wallingford, CT **2004**.

[13] S.-J. Su, H. Sasabe, Y.-J. Pu, K. Nakayama, J. Kido, *Adv. Mater.* **2010**, *22*, 3311.

[14] M. Keum, J. Han, *J. Korean Phys. Soc.* **2008**, *53*, 1580.

[15] S.-Y. Kim, J.-J. Kim, *Org. Electron.* **2010**, *11*, 1010.

[16] R. Meerheim, K. Walzer, G. He, M. Pfeiffer, K. Leo, *Proc. SPIE* **2006**, *6192*, 61920P.

[17] S.-J. Su, C. Cai, J. Kido, *Chem. Mater.* **2011**, *23*, 274.

[18] S.-J. Su, C. Cai, J. Kido, *J. Mater. Chem.* **2012**, *22*, 3447.

[19] a) G. He, M. Pfeiffer, K. Leo, M. Hofmann, J. Birnstock, R. Pudzich, J. Salbeck, *Appl. Phys. Lett.* **2004**, *85*, 3911; b) S. Watanabe, N. Ide, J. Kido, *Jpn. J. Appl. Phys., Part 1* **2007**, *46*, 1186.

[20] a) S. M. Lee, C. W. Tang, L. J. Rothberg, *Appl. Phys. Lett.* **2012**, *101*, 043303; b) J. H. Lee, J.-I. Lee, J. Y. Lee, H. Y. Chu, *Org. Electron.* **2009**, *10*, 1529.

[21] S.-J. Su, H. Sasabe, T. Takeda, J. Kido, *Chem. Mater.* **2008**, *20*, 1691.